

# Color changes in objects in natural scenes as a function of observation distance and weather conditions

Javier Romero,\* Raúl Luzón-González, Juan L. Nieves, and Javier Hernández-Andrés

Optics Department, University of Granada, Campus Universitario Fuentenueva, Fuentenueva s/n, 18071 Granada, Spain

\*Corresponding author: jromero@ugr.es

Received 18 May 2011; revised 14 September 2011; accepted 14 September 2011; posted 15 September 2011 (Doc. ID 147750); published 26 September 2011

We have analyzed the changes in the color of objects in natural scenes due to atmospheric scattering according to changes in the distance of observation. Hook-shaped curves were found in the chromaticity diagram when the object moved from zero distance to long distances, where the object chromaticity coordinates approached the color coordinates of the horizon. This trend is the result of the combined effect of attenuation in the direct light arriving to the observer from the object and the airlight added during its trajectory. Atmospheric scattering leads to a fall in the object's visibility, which is measurable as a difference in color between the object and the background (taken here to be the horizon). Focusing on color difference instead of luminance difference could produce different visibility values depending on the color tolerance used. We assessed the cone-excitation ratio constancy for several objects at different distances. Affine relationships were obtained when an object's cone excitations were represented both at zero distance and increasing distances. These results could help to explain color constancy in natural scenes for objects at different distances, a phenomenon that has been pointed out by different authors. © 2011 Optical Society of America

OCIS codes: 010.1290, 010.1310, 010.1690, 010.7295.

## 1. Introduction

Natural scenes contain a great diversity of chromaticities coming from different natural objects (mountains, terrains, forests, etc.), from artificial objects (buildings, factories, etc.), and from the sky itself. Hues such as ochre, red, and brown deriving from terrains, green and yellow from the vegetation, and blue and white from the sky are very common. Other colors belonging to fundamental hues, such as blue, green, yellow, red, and purple can be seen in flower petals, bird feathers, and insect wings and also in artificial objects.

Several authors [1–4] have studied the color gamut present in natural scenes. Nascimento *et al.* [1] described the distribution of colors measured in both

natural and urban scenes with reference to the CIE 1931 chromaticity diagram. In urban scenes the color gamut is somewhat wider due to artificial objects. In general, the natural scenes measured by Nascimento *et al.* [1] included no objects very far from the camera, and the visibility conditions were good. Hendley and Hecht [2] concluded that colors in nature show low excitation purity values, meaning that their chromaticity coordinates do not fall close to the spectrum locus and they are far from the line of the purples in the chromaticity diagram. This magnitude of purity is related to the perceptual attribute of color saturation, that is, its pure-color content in the sense of spectral color. A color becomes more saturated as its chromaticity coordinates plot nearer to the spectrum locus and less saturated as they plot closer to the area representing the white colors in the chromaticity diagram. These authors point out that saturation decreases as the distance between

the object and the observer grows, even on days with good visibility.

It is well known that the atmosphere influences our perception of the color of distant objects in natural scenes [5]. The change in color of an object observed at a distance is a consequence of the interaction between light and the different sized particles in the atmosphere, known as absorption and scattering processes. There are two ways of explaining the scattering process, depending on the size of the dominant particles present in the atmosphere. When the size of the particles is less than 10% of the wavelength of the incident light, the scattering process can be explained according to the Rayleigh theory, according to which the short wavelengths of light coming from a distant object undergo higher loss. For particle sizes of about the same size or larger than 10% of the wavelength, such as those in water vapor, the scattering process is explained using the Mie theory, according to which the dependence between light scattering and wavelength decreases [5].

When an observer looks at a distant object, we have to consider not only the direct light from the object to the observer, which undergoes scattering and absorption processes, but also the light added in the cone of vision coming from light scattered by particles in the atmosphere [5]. This component is known as airlight, which is predominantly white or bluish depending on the size of the particles in the atmosphere, and its presence leads to a loss in contrast in the perception of objects at a distance [6,7]. As a consequence of airlight, objects appear to be whitish, brighter, and have less color saturation. As the distance between the observer and the object increases, airlight becomes more important and objects appear to be less and less color-saturated, eventually approaching the color of the horizon. This effect clearly influences image contrast and can be easily discerned by looking at a distant mountain ridge. This airlight process may well have conditioned previous reports of color distribution in natural scenarios.

The loss in contrast due to airlight can be assessed by the magnitude of visibility. This magnitude is a measurement of the capacity to distinguish an object against the horizon (taken here to be the background), and it is given in terms of the limiting distance at which discernment is still possible. Visibility depends to a great extent on the predominant particle size in the atmosphere together with its density: clear air, haze, mist, fog, rain, or snow [5]. As the distance between the object and the observer increases, the object tends towards invisibility because the object and the background (horizon) become indistinguishable.

An object's bluishness is sometimes not evident due to the fact that Mie scattering can be more important than Rayleigh scattering and possibly due to some kind of ability in the human visual system to maintain the distant object's hue. Henry *et al.* [8] have shown through psychophysical experiments that in spite of the fact that distant objects appear

to be less color-saturated, the human visual system is able to discount the bluish effect and maintain the object's hue. This effect is known as atmospheric color constancy [9].

Changes in the color of objects with distance have also been qualitatively described on many occasions [10], but there seems to be nothing published about colorimetric measurements of these changes. The first objective of our work, therefore, was to address the question of how the color of objects changes according to their distance from the viewer. To this end we used a physical atmospheric model, both for clear and overcast days. The evolution of the color of objects with distance was calculated on the basis of some known experimental atmospheric parameters. Thus it was possible to ascertain color ranges at any distance.

Our second aim deals with the concept of visibility. At present, the visibility of an object is evaluated as a function of the brightness contrast between the object and background, the horizon in our case, i.e., taking into account only the human capacity to discriminate between luminances. But at the photopic level of illumination, as during the day, object perception involves color vision, so why is color not taken into account in the definition of visibility? Thus we wondered whether taking the chromaticity of the objects into account might affect our visibility measurements.

The third aim of this work relates to the constant color appearance of an object when daylight changes, that is, to color constancy. The appearance of objects does not change for different days, hours of the day, or atmospheric conditions in spite of the colorimetric changes provoked by the changes in illumination. Working with a wide range of objects, several authors [1,11–14] have found a linear relationship with a high correlation coefficient representing the pairs of excitation values for each cone photoreceptor (L, M, or S) determined for each object under daylight illumination at two different color temperatures. Foster and Nascimento [12] explain the color-constancy phenomenon based on these linear relationships. We have tested to see whether these linear relationships hold good when studying cone-excitation values for objects located at different distances. In this way, we hope to contribute to the theories based on these assumptions or make some insights into the maintenance of hue and the atmospheric color constancy of objects according to their distance from the observer, as Henry *et al.* [8] have described.

## 2. Method

To evaluate the color of an object with a spectral reflectance  $\rho(\lambda)$  in a natural scene, either directly or indirectly illuminated by the sun, and observed at a certain distance, we must assess the spectral radiance shown by the object at the location of the observer. Such spectral radiance is composed of two terms: one induced by direct light coming from the object toward the observer, which undergoes atmospheric

attenuation, and the other by added light in the observer's cone of vision due to atmospheric scattering, or airlight. The physical model that supports these assumptions is named the "dichromatic atmospheric scattering model" [15,16] and is illustrated in the schematic representation shown in Fig. 1.

According to [15–18] the object's spectral radiance observed at a distance  $d$  can be expressed as

$$L(\lambda) = L_0(\lambda) \exp(-\beta(\lambda)d) + L_\infty(\lambda)(1 - \exp(-\beta(\lambda)d)), \quad (1)$$

where  $L_0(\lambda)$  is the object's spectral radiance at zero distance,  $\beta(\lambda)$  is the extinction coefficient in the atmosphere, and  $L_\infty(\lambda)$  is the spectral radiance of the horizon. This equation supposes a homogeneous atmosphere, that is,  $\beta(\lambda)$  is taken to be the same throughout the trajectory from the object to the observer. The first term represents attenuated direct light, whilst the second one represents the airlight phenomenon.

On overcast days the light impinging upon the object comes from the whole sky dome [19,20], and now the object's spectral radiance will be

$$L(\lambda) = L_\infty(\lambda)\rho(\lambda) \exp(-\beta(\lambda)d) + L_\infty(\lambda)(1 - \exp(-\beta(\lambda)d)), \quad (2)$$

where  $\rho(\lambda)$  is the object's spectral reflectance. For this equation to hold good, it must be presumed that the object's surface exhibits Lambertian behavior and that the only light source is the sky, thus disregarding other possible sources such as light reflected by the terrain or by other objects in the scene.

On clear days, under the same assumptions made for overcast days, the following expression can be deduced [21]:

$$L(\lambda) = E_d(\lambda) \frac{\rho(\lambda)}{\pi} \exp(-\beta(\lambda)d) + L_\infty(\lambda)(1 - \exp(-\beta(\lambda)d)), \quad (3)$$

where  $E_d(\lambda)$  is the spectral irradiance upon the object illuminated by the sun.

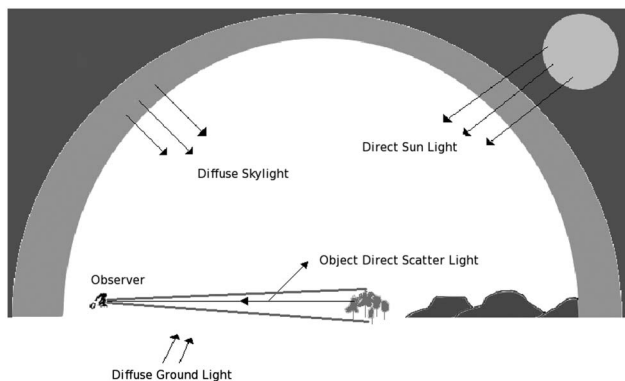


Fig. 1. Schematic representation of different light contributions.

Using Eqs. (2) and (3) the color coordinates for different objects can be obtained for different distances. These coordinates have been obtained in the CIE 1931 ( $x, y, Y$ ) and in the CIELAB color spaces [22]. The objects, of known spectral reflectance, were taken from the Munsell ColorChecker [23].

The spectral radiance of the horizon,  $L_\infty(\lambda)$ , was measured with a telespectroradiometer (SpectraColorimeter, PR-650, Photo Research Inc., Chatsworth, California). The spectral irradiance of the light illuminating the objects was measured with the same instrument at zero distance of observation and was presumed to be the same at any distance from the observer at which the object might be located, both on clear and overcast days. The spectroradiometer is affected by shot noise, as is any photodetector. A simulation of this noise, using Poisson statistics [24,25], was taken into account to study its influence on the evaluation of the chromaticity coordinates. We found that for the levels of luminance during the days in question, the effect on the assessment of the chromaticity coordinates was negligible, yielding a color difference between the measured sample and the noisy one of below 0.1 of a CIELAB unit.

The atmospheric extinction coefficient,  $\beta(\lambda)$ , was measured with a nephelometer in the CEAMA (Centro Andaluz de Medio Ambiente) laboratory [26]. The extinction coefficient is the sum of the scattering coefficient and the absorption coefficient  $\beta_{ab}(\lambda)$ , [5]. The scattering coefficient was measured at three wavelengths (450, 550, and 700 nm) [18] and extrapolated for the rest of the visibility range by obtaining the value of parameter  $u$  in the expression

$$\beta_{sc}(\lambda) \propto \frac{1}{\lambda^u}. \quad (4)$$

Parameter  $u$  is related to the amount and type of aerosols present in the atmosphere [27]. Equation (4) shows the typical spectral dependence of the scattering coefficient [5]. The  $u$  values range from 0 for dense fog to 4 for a perfectly clear atmosphere and are thus directly related to the concept of visibility in the atmosphere: on foggy days the values of  $u$  are lower, as is visibility.

The range of variation in the extinction coefficients for the days measured was between 50 and 150  $\text{Mm}^{-1}$  at 550 nm wavelength. Under the atmospheric conditions studied in this work we have assumed the single scattering approach [5]. Typical values of  $u$  for haze are between 1 and 2 [27]. The  $u$  coefficient is shown in Table 1 for the days when the measurements were made. Only one day has a coefficient with a value of  $u$  lower than 1, corresponding to a day with high dust content in the atmosphere. In the visible range, the absorption coefficient was taken to be constant and measured at 670 nm [28].

**Table 1. Measure Days, Sky Conditions, and  $u$  Coefficient**

Day (Year 2010)	Sky Condition	$u$
9 March	Clear	1.9
15 March	Clear	1.8
16 March	Clear	1.9
18 March	Overcast	1.4
19 March	Overcast	0.4
14 April	Clear	1.7
16 April	Overcast	1.9
19 April	Clear	1.7
20 April	Overcast	1.9
21 April	Clear	1.9
28 April	Clear	1.6
23 November	Overcast	1.9
24 November	Overcast	1.8
26 November	Overcast	1.6
9 December	Clear	1.3
13 December	Clear	1.6
14 December	Clear	1.5
15 December	Clear	1.5
16 December	Clear	1.6

**3. Results**

**A. Variations in an Object's Color According to Observation Distance**

Table 2 shows an example of the change in the color coordinates of an object according to the distance between it and the observer. The color coordinates are expressed in terms of CIE 1931 and CIELAB color spaces. Table 2 corresponds to a yellowish-green object on a clear hazy day (day one). As can be seen, the chromaticity coordinates change according to distance, with a tendency to stabilize at long distances. It can be deduced from Eq. (3) that this tendency moves toward the chromaticity coordinates of the horizon. For the  $a^*$ ,  $b^*$ , and  $L^*$  coordinates the tendency is to (0, 0, 100). We have taken the reference "white" in the CIELAB expressions as a perfect white reflecting surface illuminated to the same extent as the object at each distance. Table 3 shows the same object for an overcast day (day four) with a lower  $u$  value. In this case, the horizon chromaticity coordinates are reached more quickly at shorter distances. This day presented lower visibility than the previous ones. Color trend according to observation distance

**Table 2. Chromaticity Coordinate Evolution for the 6G Sample of ColorChecker DC in CIE 1931  $xy$  and CIE 1976  $L^*a^*b^*$  for Different Distances, 9 March 2010, Clear Day,  $u = 1.9$**

Distance (km)	$x$	$y$	$L^*$	$a^*$	$b^*$
0.0	0.4177	0.5098	65.59	-17.97	65.45
0.2	0.4041	0.4900	66.53	-17.35	55.13
1.0	0.3674	0.4364	69.83	-15.31	33.90
2.0	0.3420	0.3991	73.13	-13.43	21.70
5.0	0.3091	0.3511	79.83	-9.93	7.81
10.0	0.2914	0.3251	85.94	-6.98	1.59
30.0	0.2794	0.3069	94.28	-3.04	-1.30
60.0	0.2806	0.3075	97.52	-1.46	-1.10
70.0	0.2817	0.3086	98.03	-1.21	-0.99

**Table 3. Chromaticity Coordinate Evolution for the 6G Sample of ColorChecker DC in CIE 1931  $xy$  and CIE 1976  $L^*a^*b^*$  for Different Distances, 18 March 2010, Overcast,  $u = 1.4$**

Distance (km)	$x$	$y$	$L^*$	$a^*$	$b^*$
0.0	0.4092	0.5293	65.96	-14.61	65.19
0.2	0.3888	0.4873	69.15	-11.87	43.53
1.0	0.3556	0.4190	77.72	-6.26	18.49
2.0	0.3420	0.3909	83.79	-3.52	9.57
5.0	0.3302	0.3664	91.91	-1.15	2.81
14.0	0.3261	0.3548	97.96	-0.20	0.35

for an orange object in four days (two overcast and two clear) is set out in the CIE 1931 ( $x,y$ ) diagram in Fig. 2. The extremes of each of the curves correspond to the object's color at zero distance and the convergence point to the horizon color, for a long distance.

In Fig. 2 hook-shaped curves can be seen for three days, both clear and overcast. The same hook-shaped curves were obtained for the rest of the samples. If the  $u$  value were less than one, this kind of curve would not be found. Because the extinction coefficient reduces their dependence on the wavelength,  $\lambda$ , the evolution of the curves becomes an almost straight desaturation line toward the horizon chromaticity coordinates.

For the remaining days it is possible to distinguish two sections in the curves. The first, corresponding to the chromaticity coordinates of the object from 0 to middle distances, shows strong desaturation due to the airlight component. This desaturation is also affected by the wavelength dependence of the extinction coefficient. According to Eqs. (2) and (3), attenuation is higher in the short-wavelength range for light coming directly from the object (the first term of the equations). On the other hand, the airlight

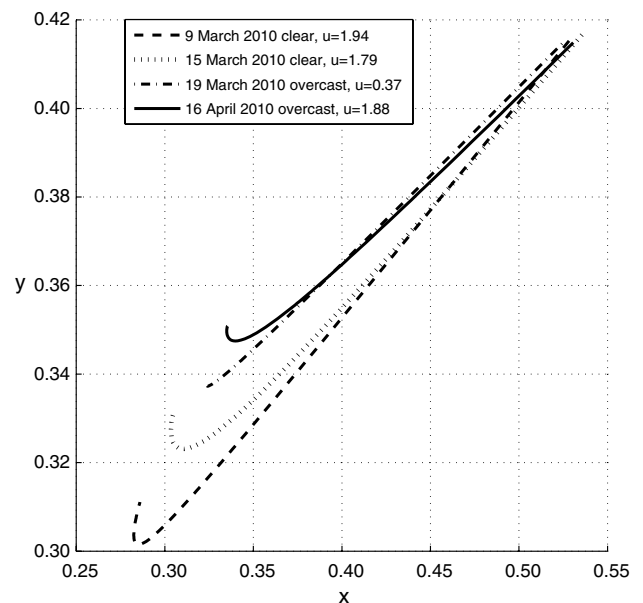


Fig. 2. Chromaticity coordinate evolution in CIE 1931 diagram for sample 4L of ColorChecker DC on four days.

component is more relevant at short wavelengths, giving a bluish component to the object's color. The result is a combination of both opponent terms, with the airlight term acquiring greater importance concomitantly with the increase in distance from the observer.

For long distances, however, the term  $\exp(-\beta(\lambda)d)$  becomes lower in value, and consequently the airlight component depends less on wavelength, resulting in the chromaticity of an object tending toward the chromaticity of the horizon, whatever its original color. Thus the second part of the curve, the bent zone, appears.

Figure 3 shows the trend of several samples on the same day in terms of the CIELAB [Fig. 3(a)] and CIE 1931 [Fig. 3(b)] color systems. Every sample chromaticity moves toward the chromaticity of the horizon, and thus it may be deduced that the color gamut in a natural scene at a long distance will be narrower than that at a short distance. Figures 4 and 5 represent the evolution of color gamut for the Macbeth ColorChecker [23] samples according to distance (Fig. 4 on a clear day and Fig. 5 on an overcast day). The color gamut for distance 0 m is similar to that found in [1] for natural scenes. The color gamut becomes smaller concomitantly with an increase in distance; this behavior is more noticeable on an overcast day, when the extinction coefficient is higher in value and the  $u$  parameter is lower than on a clear day, thus leading to lower visibility.

### B. Color and the Visibility Criterion

The visibility criterion used in the literature concerning atmospheric optics is related to the perceptual ability to distinguish an object at a certain distance against the background. It is usually based on the

maximum distance that a black object can be made out against the horizon. A black object seen at a long distance has a certain luminance due to airlight, which can be discerned or not against the horizon. The visibility criterion is based on the luminance-contrast threshold between the object and the uniform background (horizon) [5]. This criterion, therefore, is based on the perceived brightness of an object and the background and does not take into account any chromatic aspect.

Does the color of an object influence its visibility against the horizon? To address this question, the difference in lightness ( $\Delta L^*$ ), chromaticity ( $\Delta E_{a^*b^*}$ ), and color ( $\Delta E_{L^*a^*b^*}$ ) between the object and the background (horizon), calculated in terms of the CIELAB system, are represented in Fig. 6 at different distances. It can be deduced that at short distances the total color difference ( $\Delta E_{L^*a^*b^*}$ ) and the lightness difference ( $\Delta L^*$ ) are close, the relative contribution of chromaticity difference ( $\Delta E_{a^*b^*}$ ) being less important. Nonetheless, the three curves are close for long distances, the chromaticity difference being higher than the lightness difference.

Visibility as a magnitude has classically been calculated according to a luminance threshold criterion [29,30], taking the Weber's fraction  $\Delta L^*/L^*$  limiting value as 0.02. Weber's fraction measures the contrast between the object (black object) and the background. The numerator measures the luminance difference at the limit of discrimination between both, and the denominator is the background luminance. This criterion is based on psychophysical data of luminance discrimination in photopic vision. A 0.02 classical Weber's fraction is adopted [5] instead of the 0.01 usually used in psychophysical experiments under ideal observation conditions. A 0.02 value

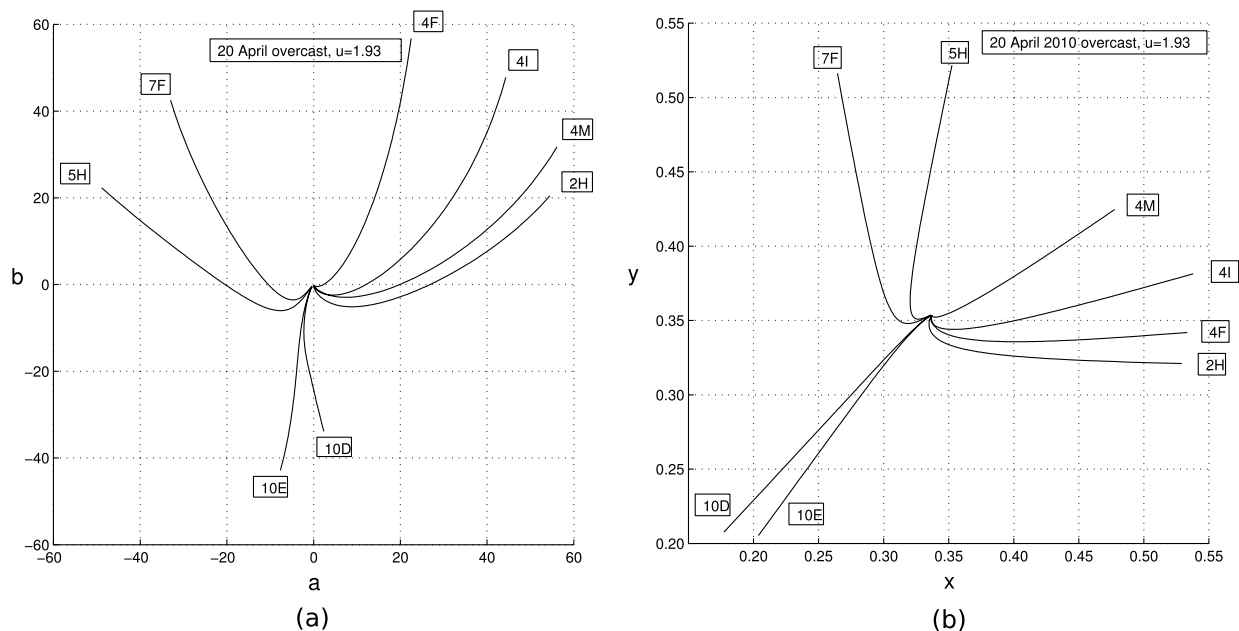


Fig. 3. Chromaticity coordinate evolution for several samples of ColorChecker DC, 20 April 2010, overcast day. (a) CIELAB ( $a^*b^*$  components) and (b) CIE 1931 ( $xy$  components) color systems.

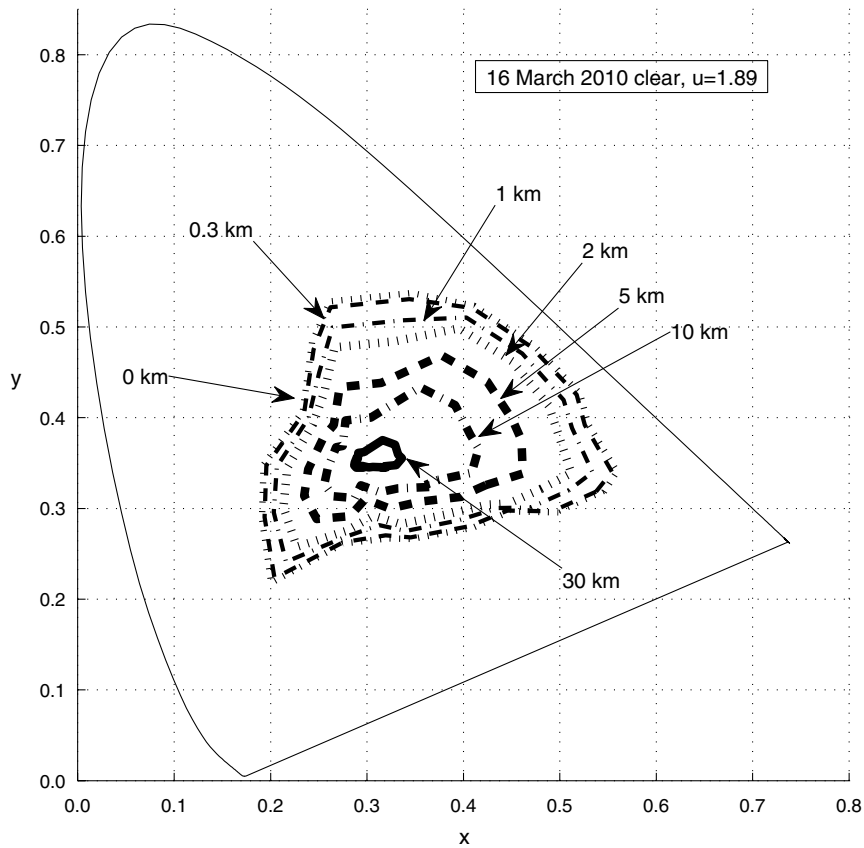


Fig. 4. Color gamut reduction as the distance increases in CIE 1931 color system ( $xy$  components), 16 March 2010, clear day.

gives a restricted visibility range, which could be advantageous in certain circumstances such as airport security.

Instead of considering a black object, we took six colored objects of different hues, and using assessed

lookup tables (see Table 4 for the results for three days) we estimated the distance at which Weber's fraction, taking lightness,  $L^*$ , as the variable, has a value close to 0.02 against the horizon. For the same distance we determined the chromaticity difference

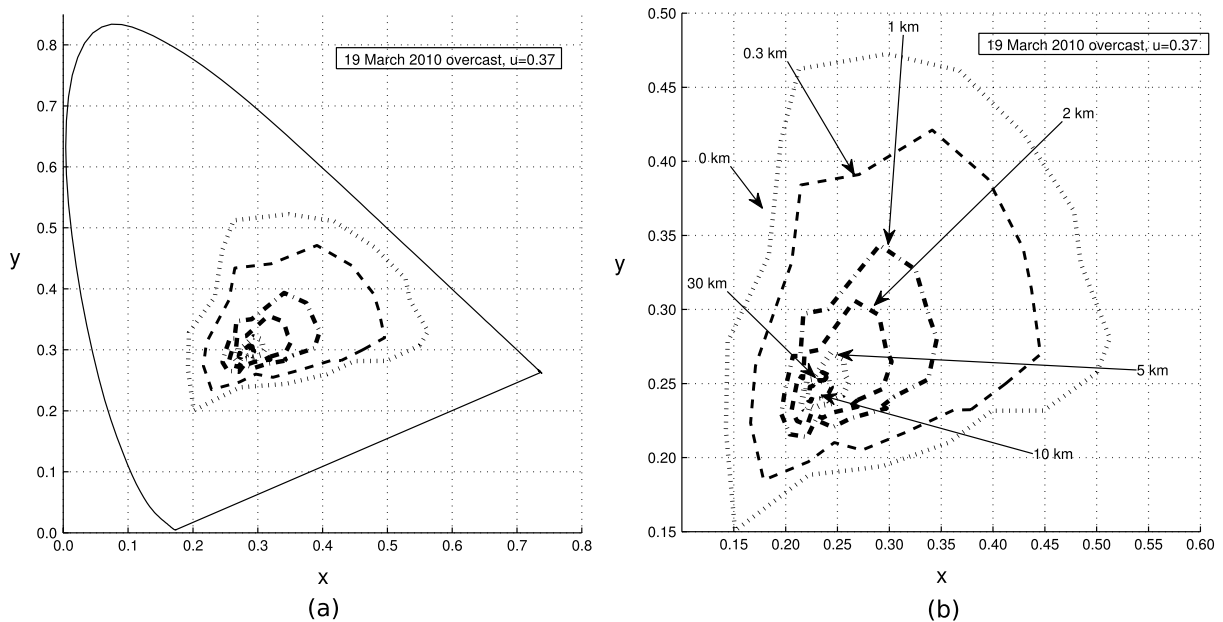


Fig. 5. (a) Color gamut reduction as the distance increases in CIE 1931 color system ( $xy$  components), 19 March 2010, overcast day; (b) enlarged version of the figure.

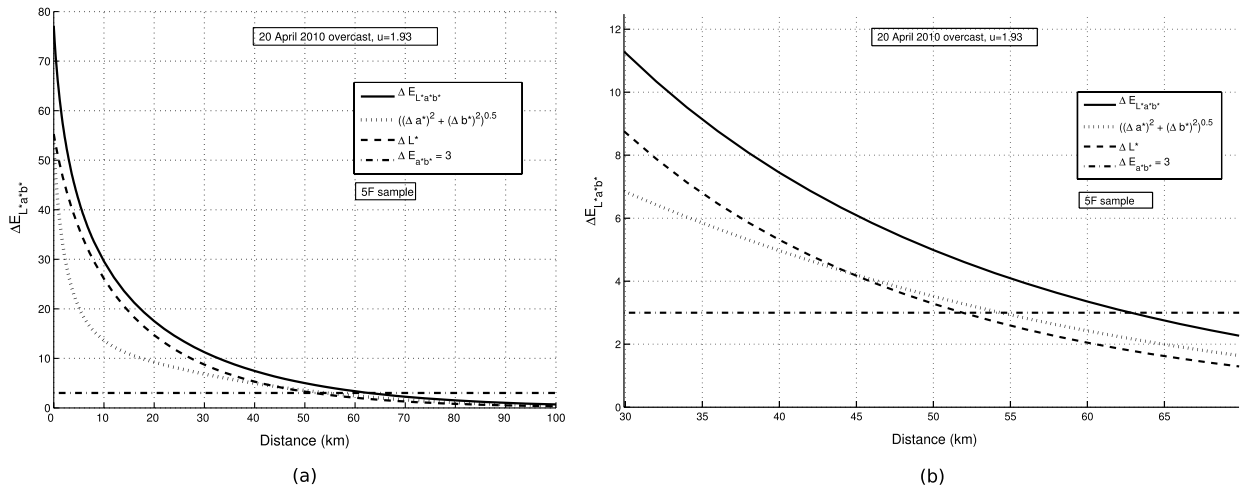


Fig. 6. Difference in lightness ( $\Delta L^*$ ), chromaticity ( $\Delta E_{a^*b^*}$ ), and color ( $\Delta E_{L^*a^*b^*}$ ) between an object and the background (horizon), calculated in terms of the CIELAB system, are shown in order to demonstrate the influence of the color of an object on its visibility against the horizon. (a) Color differences as a function of the distance for sample 5F of ColorChecker DC against the horizon, 20 April 2010, overcast day; (b) enlarged version of the figure.

between the objects and the horizon. We could then check to ascertain whether at the distance where Weber's fraction reached the discrimination threshold value between the object and the background, the color difference would still be enough to distinguish them. The answer to this query depends on accepted color tolerance. When the colors are adjacent, a color difference of one CIELAB unit is accepted. Sometimes color differences of three CIELAB units are admitted, since one CIELAB color difference is too strict [31,32].

The results set out in Table 4 show that three CIELAB color difference units and a Weber's fraction

of 0.02 are very similar in many cases. As can be seen in Table 4, however, in some cases a Weber's fraction of 0.02 corresponds to a lower value than three CIELAB color difference units, and consequently the object is indistinguishable at shorter distances than the ones specified by the classical visibility criterion.

Depending on the atmospheric conditions on the day of observation (see Table 4), the visibility of several objects is less than that assessed on the basis of the classical criteria. On the other hand, under optimum illumination conditions, such as high photopic level and an optical field of view wider than  $1^\circ$ , if we take a color tolerance close to one CIELAB unit, the distance at which the object is indistinguishable from the horizon might be much longer than the distance given by the classical visibility criterion. Thus it may be concluded that color can influence the contrast of objects against the horizon.

Table 4. Color Differences and Weber's Fraction Thresholds for Different Samples of ColorChecker DC against the Horizon, 15 March (Clear), 16 April (Overcast), and 20 April (Overcast)

Date (2010)	Sample	Distance		
		(km)	$\Delta E_{L^*a^*b^*}$	$\Delta L^*/L^*$
15 March, clear, $u = 1.8$	2C	48	3.37	0.021
	4L	44	3.06	0.021
	5F	48	3.14	0.021
	6G	42	3.65	0.022
	7F	48	3.37	0.021
	8D	48	3.40	0.022
	11E	48	3.66	0.022
	16 April, overcast, $u = 1.9$	2C	46	2.81
4L	44	2.35	0.020	
5F	46	2.84	0.022	
6G	42	2.40	0.021	
7F	46	3.02	0.022	
8D	46	3.10	0.022	
11E	48	2.63	0.020	
20 April, overcast, $u = 1.9$	2C	60	2.89	0.020
	4L	54	2.75	0.022
	5F	60	3.15	0.020
	6G	52	2.95	0.022
	7F	60	3.35	0.021
	8D	60	3.40	0.021
11E	60	3.09	0.021	

### C. Cone-Excitation Ratios and Distance

The human capacity to maintain the appearance of the color of an object under changes in illumination is known as color constancy. This holds good when daylight changes spectrally, for instance, for different phases of daylight on different days or different hours of the same day. There are various theories to explain this phenomenon [9]; one of these, called relational color constancy, is based on the constancy of the excitation ratio of the cones for the objects when the illuminant changes. When, for any specific cone receptor [33], the excitation values of several objects under a specific illuminant are represented as a function of those obtained under another illuminant, the result is a straight line with a high correlation coefficient [1]. Some color constancy theories used to develop object-recognition algorithms are also based on cone-excitation ratio constancy [9,11]. Figure 7(a) shows an example of cone-excitation ratio constancy.

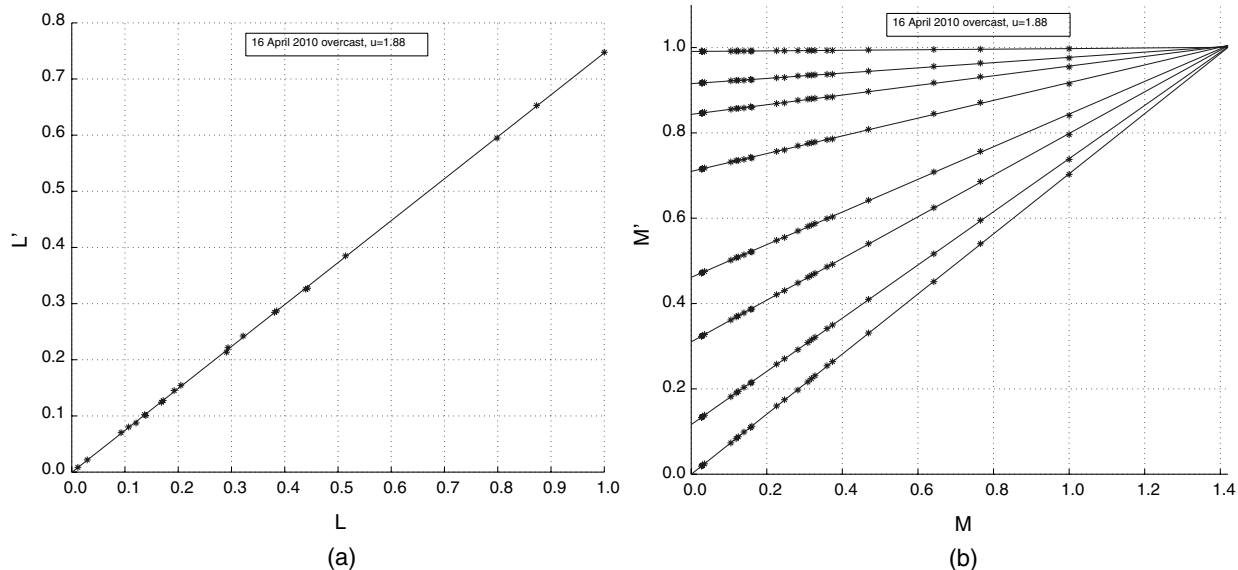


Fig. 7. Cone-excitation ratio constancy for 20 samples (1F, 2C, 2G, 2I, 2R, 4I, 4K, 5F, 5M, 5R, 6G, 6F, 6H, 7M, 9M, 10F, 10H, 11H, 11I, 11N) of ColorChecker DC, 16 April 2010, overcast day. (a) L sensor ratio constancy at zero distance, (b) M sensor ratio constancy at different distances.

The L-cone excitation under a daylight illuminant (ordinate axis) and under an equi-energetic illuminant (abscissa axis) has been represented for the samples of the Munsell ColorChecker. In this case, we considered the samples as being seen at zero distance to the observer, and so neither attenuation nor airlight were taken into account in the calculation of the values in daylight. As may be supposed, this results in a high value for the linear correlation coefficient. In Fig. 7(b) a similar example is represented for M cones, but in this case the objects were situated at increasing distances. The value of the linear correlation coefficient is also high, but the intercept is other than zero (see Table 5).

The intercept increases concomitantly with a decrease in the slope as the object gets farther and farther away from the observer. These results might be expected, because the color gamut of the object collection lessens the farther the distance, while the cone response remains much the same. This value corresponds to the cone excitation value for the horizon. The explanation for the nonzero value of the

intercept is to be found in the airlight phenomenon. The cone response at a certain distance had a value other than zero, even for a black object, the L, M, and S values of which are (0,0,0) for close distance, due to the airlight contribution. The results shown in Fig. 7 were found for each day measured and for every cone type. They can help to explain atmospheric color constancy. Henry *et al.* [8] showed hue constancy for objects observed at different distances, which can be related to the linear correlation found for the cone excitation values. Hagedorn and D'Zmura [34] related contrast constancy for objects seen in foggy conditions to an affine model to represent the light that is received from an object under foggy conditions, called a dichromatic model. In this case, we have demonstrated that this affine model also holds good when cone excitation is considered.

#### 4. Conclusions

We have studied alterations in the color coordinates of objects in natural scenes caused by atmospheric scattering according to changes in the distance of observation. Representations of the evolution of an object's color in the chromaticity diagram result in hook-shaped curves as the object moves from zero to long distances, where the object chromaticity coordinates approach the color coordinates of the horizon. This trend is the result of the combined effect of attenuation in the direct light arriving to the observer from the object and the airlight added during its trajectory. These hook-shaped curves are more pronounced when the dependence of the extinction coefficient upon wavelength is more pronounced, that is to say, on hazier days with high  $u$  values. The desaturation process observed in the color of the objects as the distance of observation increases is a result of an increase in the airlight component. Thus we can

Table 5. Data Analysis Results for Different Distances Simulated for 20 Samples (1F, 2C, 2G, 2I, 2R, 4I, 4K, 5F, 5M, 5R, 6G, 6F, 6H, 7M, 9M, 10F, 10H, 11H, 11I, 11N) of ColorChecker DC

Distance (km)	Ordinate Origin	Slope	$r^2$
0	0.000	0.669	0.999
1	0.057	0.663	0.999
3	0.162	0.563	0.999
5	0.256	0.501	0.999
10	0.447	0.374	1.000
15	0.589	0.279	0.999
20	0.695	0.208	0.999
50	0.949	0.036	0.991
$\infty$	0.998	0.002	0.956

deduce that airlight has the effect of reducing the color gamut as the distance between the observer and the object increases. Atmospheric scattering leads to a lessening of the object's visibility that can be evaluated as a color difference between the object and the background (horizon). Focusing on color difference rather than luminance difference could produce different visibility values depending on the color tolerance used.

Cone-excitation ratio constancy was assessed for several objects at different distances. Affine relations were obtained when the cone excitations produced by the objects were represented both at zero and at farther distances. The intercept increases concomitantly with distance, while the slope decreases. These results could contribute to the explanation of color constancy in natural scenes for objects at different distances, as has been mentioned by different authors [1–4,9]. In this work we have not made any estimation of noise for the cone receptors. We may ask in the future whether the inclusion of receptor-noise models might affect these results.

This work was supported by the Junta de Andalucía, Spain, under research grant P07.TIC.02642. We also thank the referees for their advice.

## References and Notes

1. S. M. C. Nascimento, F. P. Ferreira, and D. H. Foster, "Statistics of spatial cone-excitation ratios in natural scenes," *J. Opt. Soc. Am. A* **19**, 1484–1490 (2002).
2. C. D. Hendley and S. Hecht, "The colors of natural objects and terrains, and their relation to visual color deficiency," *J. Opt. Soc. Am.* **39**, 870–873 (1949).
3. G. J. Burton and I. R. Moorhead, "Color and spatial structure in natural scenes," *Appl. Opt.* **26**, 157–170 (1987).
4. M. A. Webster and J. D. Mollon, "Adaptation and the color statistics of natural images," *Vis. Res.* **37**, 3283–3298 (1997).
5. E. J. McCartney, *Optics of the Atmosphere, Scattering by Molecules and Particles* (Wiley-Interscience, 1976).
6. D. K. Lynch, "Step brightness changes of distant mountain ridges and their perception," *Appl. Opt.* **30**, 3508–3513 (1991).
7. N. S. Kopeika, I. Dror, and D. Sadot, "Causes of atmospheric blur: comment on Atmospheric scattering effect on spatial resolution of imaging systems," *J. Opt. Soc. Am. A* **15**, 3097–3106 (1998).
8. R. C. Henry, S. Mahadey, S. Urquijo, and D. Chitwood, "Color perception through atmospheric haze," *J. Opt. Soc. Am. A* **17**, 831–835 (2000).
9. D. H. Foster, "Color constancy," *Vis. Res.* **51**, 674–700 (2011).
10. M. Minnaert, *The Nature of Light and Color in the Open Air* (Dover, 1954).
11. J. Romero, D. Partal, J. L. Nieves, and J. Hernández-Andrés, "Sensor-response constancy under changes in natural and artificial illuminants," *Color Res. Appl.* **32**, 284–292 (2007).
12. D. H. Foster and S. M. C. Nascimento, "Relational colour constancy from invariant cone-excitation ratios," in *Proc. R. Soc. B* **257**, 115–121 (1994).
13. Q. Zaidi, B. Spehar, and J. DeBonet, "Color constancy in variegated scenes: role of low-level mechanisms in discounting illumination changes," *J. Opt. Soc. Am. A* **14**, 2608–2621 (1997).
14. Q. Zaidi, "Identification of illuminant and object colors: heuristic-based algorithms," *J. Opt. Soc. Am. A* **15**, 1767–1776 (1998).
15. S. G. Narasimhan and S. K. Nayar, "Chromatic framework for vision in bad weather," in *Proceedings of IEEE Conference on Computer Vision and Pattern Recognition, 2000*, Vol. 1 (IEEE, 2000), pp. 598–605.
16. S. K. Nayar and S. G. Narasimhan, "Vision in bad weather," in *Proceedings of IEEE Seventh International Conference on Computer Vision* (IEEE, 2002), pp. 820–827.
17. J. P. Oakley and B. L. Satherley, "Improving image quality in poor visibility conditions using a physical model for contrast degradation," *IEEE Trans. Image Process.* **7**, 167–179 (1998).
18. K. K. Tan and J. P. Oakley, "Physics based approach to color image enhancement in poor visibility conditions," *J. Opt. Soc. Am. A* **18**, 2460–2467 (2001).
19. S. G. Narasimhan and S. K. Nayar, "Vision and the atmosphere," in *ACM Siggraph Asia 2008 Courses* (ACM, 2008), pp. 1–22.
20. S. G. Narasimhan and S. K. Nayar, "Contrast restoration of weather degraded images," *IEEE Trans. Pattern Anal. Mach. Intell.* **25**, 713–724 (2003).
21. N. Ohta and A. R. Robertson, *Colorimetry. Fundamentals and Applications* (Wiley, 2005).
22. G. Wyszecki and W. S. Stiles, *Color Science, Concepts and Methods, Quantitative Data and Formulae* (Wiley, 1982).
23. ColorChecker DC. Chart from Gretag Macbeth Ltd. ("GMB"), 2004.
24. F. G. Smith, T. A. King, and D. Wilkins, *Optics and Photonics* (Wiley, 2007).
25. P. P. Banerjee and T. Poon, *Principles of Applied Optics* (McGraw-Hill, 1991).
26. Centro Andaluz del Medio Ambiente, Universidad de Granada, Granada, Spain, <http://atmosfera.ugr.es>.
27. M. Iqbal, *An Introduction to Solar Radiation* (Academic, 1983).
28. J. Lenoble, *Atmospheric Radiative Transfer* (A. Deepak Publishing, 1993).
29. H. Horvath, "Atmospheric visibility," *Atmos. Environ.* **15**, 1785–1796 (1981).
30. H. Horvath, "On the applicability of the Koschmider visibility formula," *Atmos. Environ.* **5**, 177–184 (1971).
31. M. J. Vrhel, R. Gershon, and L. S. Iwan, "Measurement and analysis of object reflectance spectra," *Color Res. Appl.* **19**, 4–9 (1994).
32. M. S. Drew and G. D. Finlayson, "Multispectral processing without spectra," *J. Opt. Soc. Am. A* **20**, 1181–1193 (2003).
33. P. DeMarco, J. Pokorny, and V. C. Smith, "Full-spectrum cone sensitivity functions for X chromosome linked anomalous trichromats," *J. Opt. Soc. Am. A* **9**, 1465–1476 (1992).
34. J. Hagedorn and M. D'Zmura, "Color appearance of surfaces viewed through fog," *Perception* **29**, 1169–1184 (2000).